

Heat Conduction Within Eccentric Annulus with Internal Heat Generation

Fathy M. Mahfouz and Ahmed S. Saad*

Department of Mechanical Power Engineering, Faculty of Engineering, Menoufia University, Menoufia 32511, Egypt

(*Corresponding author: ahmed.s.saad@sh-eng.menoufia.edu.eg)

ABSTRACT

Heat transfer through annular enclosures has received considerable attention due to a number of engineering applications that include thermal energy storage systems, nuclear reactors, solar energy collectors and some others. Based on the literature review, it seems that the exact solutions for heat conduction in the eccentric enclosure (that formed between two eccentric circular tubes) with internal heat generation have not been available so far. Therefore, in the present study, an exact solution for heat conduction equation in annular enclosures with uniform internal heat generation is obtained. The annular enclosure formed between two eccentric circular tubes is considered. The heat conduction process within the enclosure is mainly influenced by the enclosure geometry and internal heat generation. The solutions are obtained in terms of the temperature and local heat flux distributions along inner and outer walls of the enclosure. The solutions for dimensionless total heat transfer rates from inner and outer walls of the enclosure are also considered.

Keywords: Heat conduction; Eccentric annulus; Radius ratio; Heat flux-temperature.

1. Introduction

Heat transfer through annular enclosures has received considerable attention due to a number of engineering applications that include thermal energy storage systems, nuclear reactors, solar energy collectors and some others. In such applications heat energy transfers within the enclosure, that contains initially stagnant fluid, by one or more of the three well known modes of heat transfer. Although free convection is the main mode of heat transfer in most of such systems, the conduction mode of heat transfer becomes the dominant mode in some practical situations. The proper design of such thermal systems requires accurate prediction of the heat transfer rate in either mode and also necessitates determination of the condition of mode change.

Several previous theoretical and experimental studies have investigated heat transfer within different shapes annular enclosures (see for example [1–14]. In the case of pure conduction heat transfer in annular enclosures little work has been found. Exact solution for conduction heat transfer from two adjacent spheres without heat generation has been obtained by Alassar and Alminshawy [15] while exact solution for conduction heat transfer between two eccentric spheres with internal heat generation was obtained by Alassar [16]. Ayhan and Cemil [17] obtained exact solution of the heat conduction equation in eccentric spherical enclosures. Recently, Mahfouz [18] has

obtained the exact solution of heat conduction equation in elliptic enclosure.

Based on the literature review, it seems that the exact solutions for heat conduction in the eccentric enclosure (that formed between two eccentric circular tubes) with internal heat generation have not been available so far. Therefore, this piece of work aims to develop an exact solution for heat conduction problem in eccentric enclosures with internal heat generation. Moreover, this work aims to shed some light on some heat transfer characteristics associated with such heat conduction problems.

Beside considering the exact solution, the numerical solution of the problem is provided for the sake of comparison. The exact and numerical solutions are presented in terms of the temperature and local heat flux distributions along the walls of the enclosure. In the case of the enclosure formed between two eccentric circular tubes the geometry of the enclosure is determined in terms of the eccentricity and radius ratio of the two tubes.

2. Problem formulation

Figure 1 shows the physical domain and coordinate system for an eccentric enclosure. The eccentric enclosure is formed between two long eccentric circular tubes. Heat energy is generated within the enclosure at steady rate of q_v and then transfers through the annulus by conduction and dissipates to the surrounding environment. The temperatures of

inner and outer surfaces of the enclosure are kept uniform at T_i and T_o , respectively, with $T_i > T_o$. The thermal field in the enclosure develops with time till reaching steady state condition after a period of time. The numerical solution is obtained by solving the time dependent conduction equation till reaching the steady state conduction. Assuming constant physical properties of the stagnant fluid (material) in the enclosure the dimensionless time dependent conduction equation can be written in Cartesian coordinates as:

$$\frac{\partial \phi}{\partial t} = \left(\frac{\partial^2 \phi}{\partial x^2} + \frac{\partial^2 \phi}{\partial y^2} \right) + G \quad (1)$$

Where $x = x' / R_i$, $y = y' / R_i$, $t = \tau \alpha / R_i^2$

$$\phi = (T - T_o) / (T_i - T_o); G = \frac{R_i^2 q_v}{k(T_i - T_o)}$$

(2)

where τ is the time, T is the temperature, α is the thermal diffusivity, k is thermal conductivity and q_v is the rate of heat generation per unit volume. R_i is the radius of the inner tube. G is the heat generation parameter.

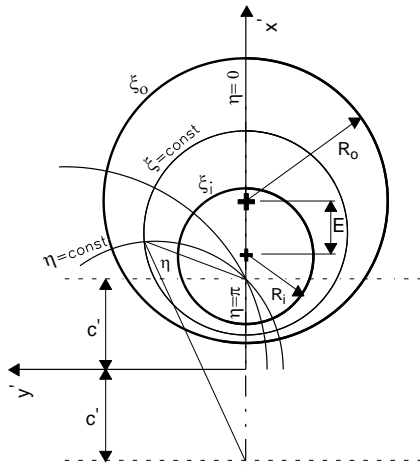


Figure 1- Physical domain and coordinate system.

3. Solution procedure

For proper exact and numerical treatment of the problem, an appropriate orthogonal coordinate transformation should be used. In case of eccentric enclosure, the bipolar coordinates ξ, η are used

These coordinates are defined as :

$$x = -c \sinh(\xi) / (\cosh \xi - \cos \eta),$$

$$y = c \sin(\eta) / (\cosh \xi - \cos \eta).$$

Using above transformation eq. (1) reads:

$$\frac{\partial \phi}{\partial t} = \frac{1}{J} \left(\frac{\partial^2 \phi}{\partial \xi^2} + \frac{\partial^2 \phi}{\partial \eta^2} \right) + G \quad (3)$$

Where,

$J = x_\xi y_\eta - y_\xi x_\eta$ is the Jacobian of coordinate transformation matrix.

In the new coordinates, the steady boundary conditions can be expressed as $\phi = 1$ on $\xi = \xi_i$ and $\phi = 0$ at $\xi = \xi_o$ where ξ_i and ξ_o define the inner and outer surfaces of the eccentric enclosure as $\xi_i = \sinh^{-1}(-c)$ and $\xi_o = \sinh^{-1}(-c/Rr)$, $c = \frac{1}{2e} \sqrt{(1-e^2)[(1+Rr)^2 - e^2(Rr-1)^2]}$,

$Rr = R_o / R_i$, is the radius ratio and $e = E / (R_o - R_i)$ is the dimensionless eccentricity.

The solution proceeds by assuming the distribution of dimensionless temperature as an exact function represented in terms of Fourier series as:

$$\phi(\xi, \eta, t) = \frac{1}{2} H_o(\xi, t) + \sum_{n=1}^N H_n(\xi, t) \cos(n\eta) \quad (4)$$

where H_o and H_n are the Fourier coefficients and N represents the number of terms considered in the Fourier series. Substitution of ϕ defined in (4) in eq. (3) and integrating the equation (after multiplying by $1, \cos n\eta$, one at a time) from 0 to 2π results in the following two differential equations:

$$a_o \frac{\partial H_o}{\partial t} + \sum_{n=1}^N a_n \frac{\partial H_n}{\partial t} = \frac{\partial^2 H_o}{\partial \xi^2} + 2a_o G \quad (5a)$$

$$a_o \frac{\partial H_n}{\partial t} + \frac{1}{2} \frac{\partial H_o}{\partial t} a_n + \frac{1}{2} \sum_{m=1}^N \frac{\partial H_m}{\partial t} (a_{n+m} + a_{|n-m|}) = \left(\frac{\partial^2 H_n}{\partial \xi^2} - n^2 H_n \right) + a_n G \quad (5b)$$

$$\text{Where; } a_o = 4c^2 \frac{b^2(b^2+1)}{(b^2-1)^3}$$

$$; b = e^{-\xi} a_n = 8c^2 \frac{b^2[2+(n+1)(b^2-1)]}{b^n(b^2-1)^3}$$

The steady boundary conditions for all Fourier functions presented in equation (5) can be expressed as:

$$-\text{At } \xi = \xi_i \quad H_n = 0, \quad H_o = 2 \quad (6a)$$

$$-\text{At } \xi = \xi_o \quad H_n = 0, \quad H_o = 0 \quad (6b)$$

Eqs. 5a and 5b along with the boundary condition (6) can now be solved to give H_o and H_n which are then used to give the temperature distribution.

4. Numerical solution

The numerical analysis proceeds further by discretizing equations 5a-b using Crank-Nicolson finite difference scheme. The discretization is carried out over uniform grids in ξ direction and with equal time steps till reaching the steady state solution. The time step is selected very small to ensure the accuracy of the numerical scheme. The resulting tri-diagonal

system of equations has been solved by Tri-Diagonal Matrix Algorithm, TDMA.

4.1. Analytical solution

Setting the local time derivatives in eqs. (5a and 5b) to zero and using boundary conditions (6), the steady state analytical solution of dimensionless temperature distribution is found as:

$$\begin{aligned} \phi(\xi, \eta) &= \frac{-Gc^2}{b^2 - 1} + \frac{1}{2}(k_1\xi + k_2) \\ &+ \sum_{n=1}^{n=N} \left(k_{3n} b^n + k_{4n} b^{-n} - \frac{2Gc^2}{b^n(b^2 - 1)} \right) \cos(n\eta) \\ k_1 &= \frac{2}{\xi_i - \xi_o} + \frac{2Gc^2}{\xi_i - \xi_o} \left(\frac{1}{b_i^2 - 1} - \frac{1}{b_o^2 - 1} \right) \\ k_2 &= \frac{2Gc^2}{b_o^2 - 1} - k_1\xi_o, \quad k_{4n} = -k_{3n} b_i^{2n} + \frac{2Gc^2}{b_i^2 - 1} \\ k_{3n} &= \frac{2Gc^2}{b_o^{2n} - b_i^{2n}} \left(\frac{1}{b_o^2 - 1} - \frac{1}{b_i^2 - 1} \right) \end{aligned}$$

4.2. Heat transfer parameters

After obtaining the numerical and analytical temperature distributions, the heat transfer characteristics are easily determined. The heat transfer results are presented in terms of dimensionless local heat flux distribution along inner and outer walls and dimensionless total heat transfer rates from inner and outer walls.

The dimensionless local heat flux at the inner and outer walls are defined as:

$$\begin{aligned} \bar{q}_o &= q_o P_o / \pi k \Delta T_{ref} \quad \bar{q}_i = q_i P_i / \pi k \Delta T_{ref} \\ q_o &= -k(\partial T / \partial S_n)_o \quad \text{where } P_i \quad q_i = -k(\partial T / \partial S_n)_i \end{aligned}$$

and P_o are the perimeters of the inner and outer walls. S_n is the local direction of local heat flux normal to the wall. $\Delta T_{ref} = T_i - T_o$ is the reference temperature difference.

Defining the dimensionless rate of heat transfer as

$$Q = \frac{1}{k \pi (T_i - T_o)} \int_0^P q \, dP, \quad \text{where } P \text{ is the perimeter.}$$

The dimensionless rate of heat transfer at inner and outer walls can be expressed as:

$$Q_i = - \left(\frac{\partial H_o}{\partial \xi} \right)_i; \quad Q_o = - \left(\frac{\partial H_o}{\partial \xi} \right)_o \quad (9) \quad \text{The}$$

application of the first law of thermodynamics entails that in the steady state condition:

$$Q_o - Q_i = \int q_v \, dV = Q_{tot}. \quad \text{It should be noted that the value of } Q_o \text{ is always positive, meaning that heat transfer dissipates from the outer wall with and without heat generation while the value and sign of } Q_i$$

depends on the heat generation parameter G. The value of G above which the heat dissipates from the inner wall is found from the analytical solution as:

$$G^* = \frac{1/c^2}{2(\xi_i - \xi_o)b_i^2/b_{ii}^2 - 1/b_{ii} + 1/b_{oo}} \quad (10)$$

where $b_{ii} = b_i^2 - 1$, $b_{oo} = b_o^2 - 1$

The critical value for G as it appears in eq. (10) depends only on the annulus geometry parameters Rr and e .

5. Results and discussion

Before proceeding to produce the final results, the exact and numerical results for steady state solutions of some test cases were obtained and compared with the well-known exact solutions for some special cases. The comparison with well known exact solution for conduction in the concentric enclosure with and without internal heat generation has shown almost identical results. Moreover, the obtained exact solution for dimensionless heat rate by conduction (under only temperature difference between the two walls) within eccentric enclosure without heat generation is deduced as:

$$Q = 2 / \cosh^{-1} \left(\frac{1 + Rr^2 - e^2(Rr - 1)^2}{2Rr} \right) \quad (11)$$

Which is the same as that presented in [13] in terms of average conduction Nusselt number.

Figure 2 shows a sample of numerical results in case of no heat generation, $G=0$ and in case of heat generation at $G=2$. The figure shows the time variation of heat transfer rates to/from inner and outer walls. In case of $G=0$ the heat rate from inner wall decreases with time while the heat dissipated from the outer wall increases with time till it almost equals that of inner wall at the steady state. While in case of $G=2$ the steady state heat rate from inner walls is negative, meaning that this heat dissipates from the wall, while the heat that dissipates from the outer wall increases continuously till reaching the steady state value. The figure also shows that the steady state analytical solutions are almost identical to the numerical ones.

Table 1 shows the steady heat transfer rates from the inner and outer walls at $Rr=2.5$ and $e=0.5$ for different values of heat generation parameter, $G=0, 0.5, 2, 5$. The table shows that in case of no heat generation, $G=0$, the heat transfer rate from the two walls, which in this case is due to temperature difference between the two walls, is positive and equal to each other which means that the heat enters the annulus from inner wall and leaves or dissipates from the outer wall. In case of $G=0.5$, the heat rates are still positive which means that the heat is still entering the enclosure through the inner wall and dissipates from the outer wall after adding the heat generated in the enclosure. While in cases of $G=2$ and 5 , the table indicates that the heat is dissipating from the two walls. It can be inferred from

these results that there would be a critical value for G between $0.5 < G^* < 2$ above which heat conduction starts dissipating from the inner wall. This value is obtained from eq. (10) and equal to $G^* = 1.408$ for this particular case.

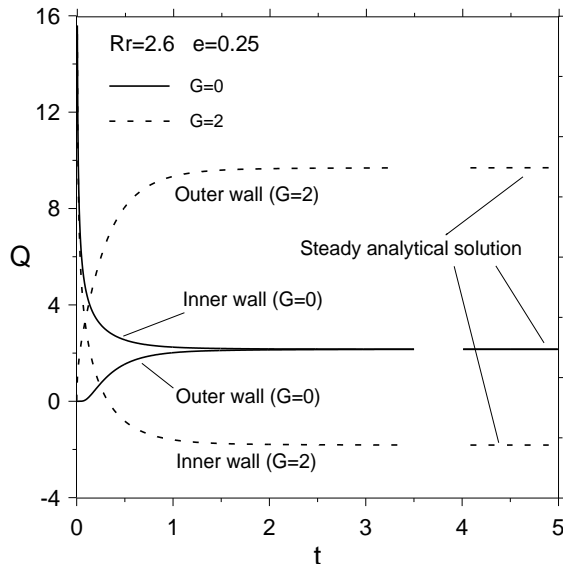


Figure 2- Time variation of numerical dimensionless heat transfer rates from inner and outer walls.

Table 1- Heat rates Q_i and Q_o for eccentric enclosure ($e = 0.5$ $Rr = 2.5$)

Q	G = 0	G = 0.5	G = 2	G = 5
Q_i	2.499	1.612	-1.051	-6.377
Q_o	2.499	4.237	9.449	19.872
Q_{tot}	0	2.625	10.5	26.249

Figure 3 shows the temperature distribution in the annulus gap along the line of $\theta = 0$ for the case of $e = 0.4$ and $Rr = 2.6$ and at different values of G . The figure shows that at $G = 0$ the temperature gradient is negative at the two walls which indicates that local heat enters the enclosure from the inner wall and dissipates from the outer wall. With presence and increase of internal heat generation parameter G the figure shows that the temperature within the enclosure along line of $\theta = 0$ increases, attaining maximum value and establishing positive temperature gradient at the inner wall and negative gradient at the outer wall. Such a temperature distribution means that the heat flux (and thus heat transfer) dissipates from the two walls. The figure also shows that the position of maximum temperature moves towards the outer wall as G increases.

Figure 4 shows the dimensionless heat flux distribution along inner wall (Fig. 4a) and outer wall (Fig. 4b) for the same cases presented in Fig. 3. It can be seen that as G increases the absolute value of heat flux increases at the same point (i. e same θ) on the wall. It can be also observed that in case of $G = 0$ the

heat flux is positive along the two walls, implying that the heat enters into the enclosure from the inner wall and dissipates from the outer wall. while for $G = 2, 6, 10$ the heat flux is negative along the inner wall but positive along the outer wall which means that for these later cases the heat dissipates from the two walls. It can be also inferred from Fig.3 that the critical value for G lies between $0 < G < 2$. This value for this particular case is equal to $G^* = 0.8445$.

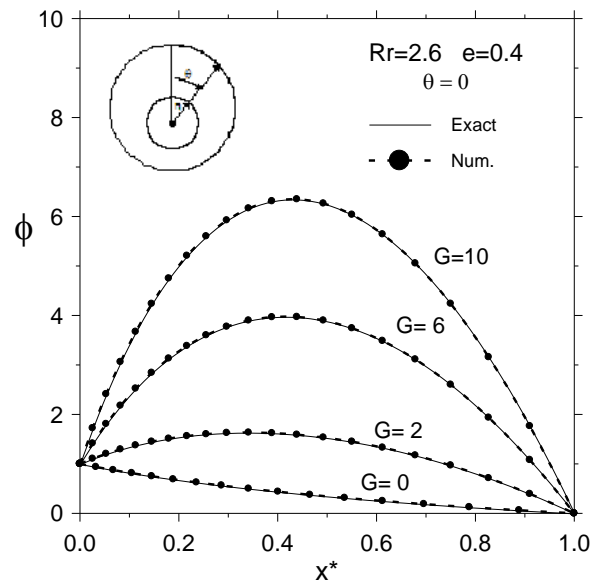
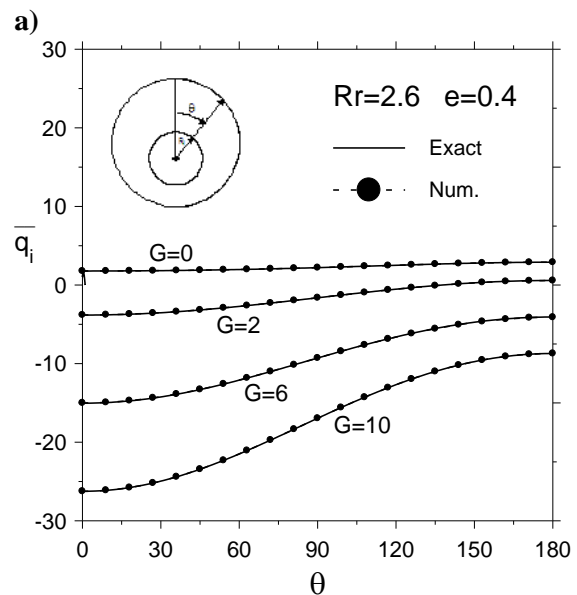


Figure 3- Distribution of dimensionless temperature in the gap along line of $\theta = 0$ and at different values of G .



b)

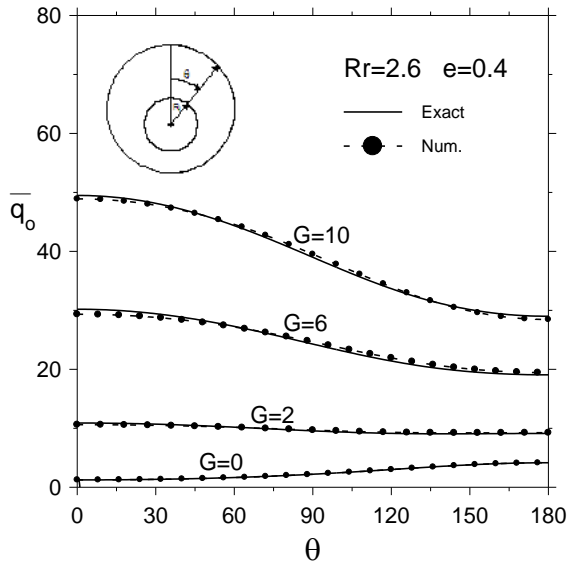


Figure 4- Heat flux along a) inner wall; b) outer wall at $Rr=2.6$, $e=0.4$ and at different values of G .

Figure 5 presents the isotherms pattern for the case of ($G=10$, $Mr=2.5$ and at different values of Ar_i , ($Ar_i=0.005, 0.35, 0.7, 0.998$). The case of $Ar_i=0.005$ represents the case of an enclosure between a flat plate and the surrounding elliptic tube while the case of $Ar_i=0.998$ approximates the case of concentric annulus. The figure clearly shows once more that the analytical solution of temperature distribution (right) is almost identical to numerical solution (left). The formation of sub-closed contours is only observed in the wide parts of the annulus near $\theta=90$ while such contours do not appear in the narrow parts near $\theta=0$.

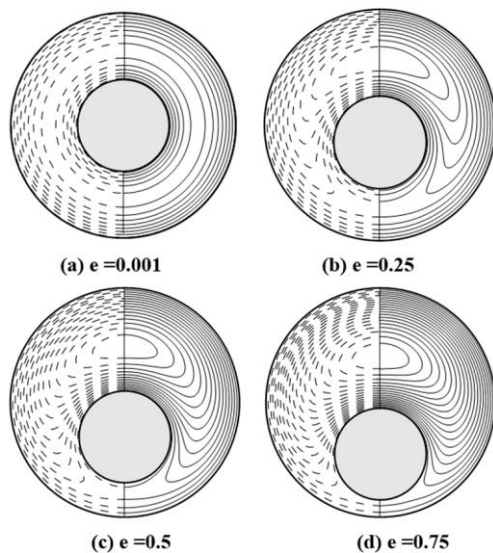


Figure 5- Patterns of exact isotherms (right) and numerical isotherms (left) for the case of eccentric enclosure at $G=10$, $Rr=2.5$ and a) $e=0.001$ (almost concentric annulus), b) $e=0.25$, c) $e=0.5$, d) $e=0.75$.

The effect of geometry on heat rates Q_i and Q_o is presented in Tables 2, 3. Table 2 shows the effect of Ar_i on the rate of heat transfer from the two walls and the total heat transfer rate in case of $G=10$, $Mr=2.6$ while Table 3 shows the effect of Mr on heat rates in case of ($G=5$, $Ar_i=0.6$). Presented in the two tables the critical value G^* for each geometry (Mr, Ar_i). Table 2 shows that for the same Mr as Ar_i increases the heat dissipated from the inner wall increases while that from the outer wall decreases and the total heat rate decreases. The increase of Ar_i at same Mr decreases the total volume of the enclosure and thus decreases the total heat generation. Table 3 indicates that for the same Ar_i as Mr increases the heat dissipated from the two walls increases as well as total heat rate. The increase of Mr for the same Ar_i increases the total volume of the enclosure and thus increases the total heat rate.

Table 2- Heat rates Q_i and Q_o for eccentric enclosure ($G=4$, $Rr=2.5$)

Q	e=0.001	e=0.25	e=0.5	e=0.75
Q_i	-5.276	-5.120	-4.601	-3.409
Q_o	15.723	15.879	16.398	17.590
Q_{tot}	20.999	20.999	20.999	20.999

Table 3- Heat rates Q_i and Q_o for eccentric enclosure ($G=6$, $e=0.4$)

Q	Rr=1.5 $G^*=10.052$	Rr=2.7 $G^*=1.043$	Rr=3.5 $G^*=0.517$	Rr=4 $G^*=0.371$
Q_i	2.167	-10.378	-18.299	-23.610
Q_o	9.667	27.362	49.200	66.389
Q_{tot}	7.500	37.740	67.499	89.999

6. Conclusion

Exact and numerical solutions for steady heat conduction in the enclosure between two long isothermal eccentric tubes with uniform internal heat generation are obtained. The solutions are obtained in terms of the dimensionless temperature and local heat flux distributions. The study has shown that the numerical results are in excellent agreement with the analytical results.

7. Nomenclature

- c Half distance between the two poles of Bi-polar coordinates
- E Eccentricity
- e Dimensionless eccentricity $=E/(R_o - R_i)$
- G Heat generation parameter
- H_o, H_n Fourier coefficients

F. M. Mahfouz and Ahmed S. Saad “Heat Conduction Within Eccentric Annulus with Internal Heat Generation”

k	Thermal conductivity
R _r	Radius ratio = (R_o / R_i)
t	Dimensionless time
T	Temperature
x, y	Dimensionless Cartesian coordinates

Greek symbols

α	Thermal diffusivity
ϕ	Dimensionless temperature = $T - T_o / \Delta T_{ref}$
η, ξ	Bi-polar coordinates
τ	Time

Subscripts

i	At the inner tube surface
o	At the outer tube surface

8. References

- [1] Chiu, C.P., Shich, J.Y. and Chen, W.R., 1999, “Transient Natural Convection of Micropolar Fluids in Concentric Spherical Annuli”, *Acta Mech.* 132, pp. 75–92.
- [2] Mahony, D.N., Kumar, R. and Bishop, E.H., 1986, “Numerical Investigation of Variable Property Effects on Laminar Natural Convection of Gases Between Two Horizontal Isothermal Concentric Cylinders,” *ASME J. of heat transfer*, 108, pp. 783–789.
- [3] El-Saden, M.R., 1961, “Heat Conduction in an Eccentrically Hollow, Infinitely Long Cylinder with Internal Heat Generation”, *ASME J. of heat transfer*, 83, pp 510–512.
- [4] Kuehn T. H., and Goldstein, R. J., 1978, “An Experimental Study of Natural Convection Heat Transfer in Concentric and Eccentric Horizontal Cylindrical Annuli,” *ASME J. of heat transfer*, 100, pp. 635–640.
- [5] Farouk, B. and Güçeri, S. I., 1982, “Laminar and Turbulent Natural Convection in the Annulus Between Horizontal Concentric Cylinders,” *ASME J. of heat transfer*, 104, pp. 631-636.
- [6] Hessami, M.A., Pollard, A., Rowe, R.D. and Ruth, D.W., 1985, “A Study of Free Convective Heat Transfer in a Horizontal Annulus with a Large Radii Ratio,” *ASME J. of heat transfer*, 107, pp. 603-610.
- [7] Pepper, D. W. and Cooper, R. E., 1983, “Numerical Solution of Natural Convection in Eccentric Annulus,” *AIAA*, 21, pp. 1331-1337.
- [8] Wang S., 1995, “An Experimental and Numerical Study of Natural Convection Heat Transfer in Horizontal Annuli Between Eccentric Cylinders,” *J. of Thermal Science*, 4(1), pp. 38-43.
- [9] Kumar, R., 1988, “Study of Natural Convection in Horizontal Annuli,” *Int. J. Heat Mass Transfer*, 31 (6), pp. 1137–1148.
- [10] Mahfouz, F. M., 2011, “Buoyancy Driven Flow Within an Inclined Elliptic Enclosure” *Int. J. of Thermal Sciences*, 50, pp. 1887–1899.
- [11] Mahfouz, F.M., 2012, “Heat Convection Within an Eccentric Annulus Heated at Either Constant Wall Temperature or Constant Heat Flux”, *ASME J. of heat transfer*, 134(8), 082502(1-9).
- [12] Mahfouz, F. M., 2012, "Natural Convection Within an Eccentric Annulus at Different Orientations", *AIAA, Journal of Thermophysics and Heat Transfer*, 26(4), pp. 665-672, 2012.
- [13] Bergman L., Lavine, A. S., Incropera, F. P., Dewitt, D. P., 2011, "Introduction to Heat Transfer", 6th edition John Wiley & Sons, Inc.
- [14] Imtiaz, H and Mahfouz, F. M., Heat transfer within an eccentric annulus containing heat generating fluid, *Int. J. Heat and Mass Transfer*, 121, 845-856, 2018.
- [15] Alassar, R.S. and Alminshawy, B.J. 2010, “Heat Conduction From two Spheres”, *AIChE J.* 56(9), pp. 2248–2256.
- [16] Alassar, R.S, 2011, “Conduction in Eccentric Spherical Annuli”, *Int. J. of Heat and Mass Transfer* 54 (2011) 3796–3800.
- [17] Y. Ayhan, K. Cemil, Exact solution of the heat conduction equation in eccentric spherical annuli, *Int. J. of Thermal Sciences* 68 (2013) 158-172.
- [18] F.M. Mahfouz, Heat conduction within elliptic enclosure with internal heat generation, *Engineering Research Journal*, 43(2) pp. 93-98, 2020.